Development of magnetic levitation system with position and orientation control

Siti Juliana Abu Bakar[1], Koay J-Shenn[2], Patrick Goh[2], Nur Syazreen Ahmad[2]
[1]Centre for Electrical Engineering Studies, Universiti Teknologi MARA, Penang, Malaysia
[2]School of Electrical and Electronic Engineering, Universiti Sains Malaysia, Penang, Malaysia

Article Info

ABSTRACT

This work demonstrates the design and development of a magnetic levitation (MagLev) system that is able to control both the position and orientation of the levitated object. For the position control, a pole placement method was exploited to estimate parameters of the proportional integral derivative (PID) controller. In addition, the MagLev was constructed using a pair of electromagnets, two infrared (IR) receiver-emitter pairs and a servo motor to allow the orientation of the object to be controlled. The proposed controller was programmed in a LabVIEW environment, which was then compiled and deployed into an embedded NI myRIO board. Experimental results demonstrated that the proposed method was able to achieve a zero steady-state orientation error when the object was rotated from $0°$ to $\pm 90°$, a steady-state position error of 0.3 cm without rotation, and steady-state position errors of no greater than 1.2 cm with rotation.

Corresponding Author:

Nur Syazreen Ahmad
School of Electrical and Electronic Engineering, Universiti Sains Malaysia
14300 Nibong Tebal, Penang, Malaysia
Email: syazreen@usm.my

1. INTRODUCTION

Magnetic levitation (MagLev) is technique to hold an object aloft by continually adjusting the strength of magnetic field produced by electromagnets. The role of the electromagnets is to generate a time-varying magnetic field that can either attract the object from above or repulse the object from below. MagLev technology is used to eliminate mechanical contact in order to alleviate friction between stationary and active parts in the system, which can eventually reduce maintenance costs and increase efficiency. The technology has attracted a wide field of applications such as high-speed trains [1]-[3], mineral measurement methods [4], plastic shrinkage void detection [5], energy harvesting [6], [7], and disease diagnostics [8]-[10].

In order to levitate an object using electromagnetic force, a feedback loop is typically present. In this case, a sensor is used to locate the object and transmit the data to the controller, which is in charge of controlling the current flowing through the coil. An electromagnet force is then generated to keep the object levitating in the desired location. As is extensively discussed in the literature, controlling the object's position is a challenging task as the MagLev system is inherently nonlinear and unstable. Plus, the equilibrium position is greatly influenced by uncertainties of the proximity sensors and magnetic field strength [11], [12]-[14]. In some cases where the uncertainties are large but statistical such as those used in high-speed trains, Gaussian process is required to extract the dynamic properties of the systems [15]-[17].

Various control methods have been proposed to stabilize the system such as proportional integral derivative (PID) [18], linear quadratic regulator (LQR) [19], and sliding mode control (SMC) [20], [21]. Nev-

ertheless, parameterization of the controllers has always been a great challenge as many modern optimal control techniques are either not directly applicable to unstable systems [22] or require perfect knowledge of the state variables. An alternative method using grey wolf optimization is proposed in [23] to obtain optimal parameters for PID and SMC. In another work presented in [24], both ant colony optimization and the Ziegler–Nichols tuning method are used to parameterize the PID controller. Nonlinear control methods such as fuzzy logic (FL) [25], [26] and neural network (NN) [27]-[29] can be advantageous due to their adaptive and self-learning capabilities. In [30]-[32] for instance, the PID and FL are combined to form a Fuzzy-PID controller to improve the MagLev's position control performance. Tang *et al.* [26] proposed an NN compensation control method based on fuzzy inference to reduce the overshoot of the position control system. Rubio *et al.* [33], the NN is used not only to control the position, but also to model the MagLev. Despite the aforementioned advantages, applications of nonlinear control methods will increase the complexity of the closed-loop which can consequently drive the system to the unstable state when perturbed.

While many control strategies have been suggested in previous studies, most of them are either limited to simulations or are only applicable for position control. To the best of the authors knowledge, controlling the orientation of the levitated object remains underexplored, although it is equally crucial particularly in microautomation such as orienting objects for assembly, sorting and positioning components in a 3D space [34], and mask and optical system alignment in semiconductor manufacturing [35]. In this work, we demonstrate the design and development of a MagLev system that is able to control both the position and orientation of the levitated object. For the position control, a pole placement method was exploited to estimate parameters of the PID controller. In addition, the MagLev was constructed using a pair of electromagnets, two infrared (IR) receiver-emitter pairs and a servo motor to allow the orientation of the object to be controlled. The proposed controller was programmed in a LabVIEW environment, which was then compiled and deployed into an embedded NI myRIO board. Experimental results demonstrated that the proposed method was able to achieve a zero steady-state orientation error when the object was rotated from $0°$ to $\pm 90°$, a steady-state position error of 0.3 cm without rotation, and steady-state position errors of no greater than 1.2 cm with rotation.

2. METHOD

2.1. MagLev architecture

The proposed structure of the MagLev is shown in Figure 1. It consists of an NI myRIO as the main controller, a servo motor holding two separate electromagnets, an amplifier to provide sufficient voltage for each electromagnet, and an infrared emitter-receiver pair (IR LED and IR photodiode) to measure the position of the levitated object. The proposed structure does not just allow both the control of position and orientation of the levitated object, but also prevents unnecessary self-rotation.
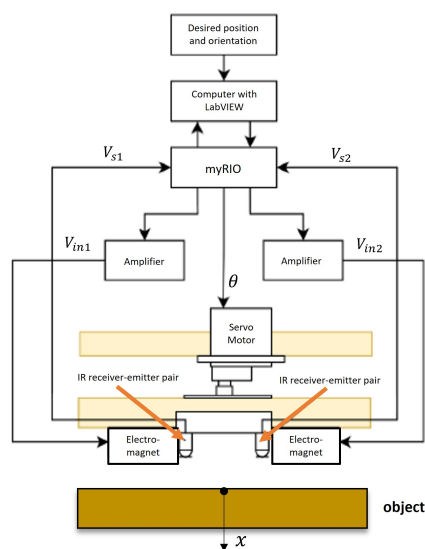

Figure 1. Proposed structure of the MagLev system

The schematic diagram of the MagLev is depicted in Figure 2 which was designed in NI Multisim software. To power the electromagnets, a 12 V voltage is required. Therefore, an amplifier is required to amplify the 5 V output from the myRIO board. The amplifier consists of a non-inverting op-amp with the amplification gain of 2.4, followed by a unity current buffer as shown in Figure 2(a).

Figure 2(b) shows the circuit for the sensing part where each IR sensor is connected to analog input pin of the myRIO. For the orientation control, a servo motor is connected to DIO3/PWM0 pin of the MSP connector C as shown in Figure 2(c). Figure 3 depicts the actual MagLev system; the servo motor is mounted on top of the structure, while the electromagnets and the sensors are mounted on a platform that the servo motor holds. The amplifier and sensor circuits are built on the breadboard as shown at the bottom part of the figure.
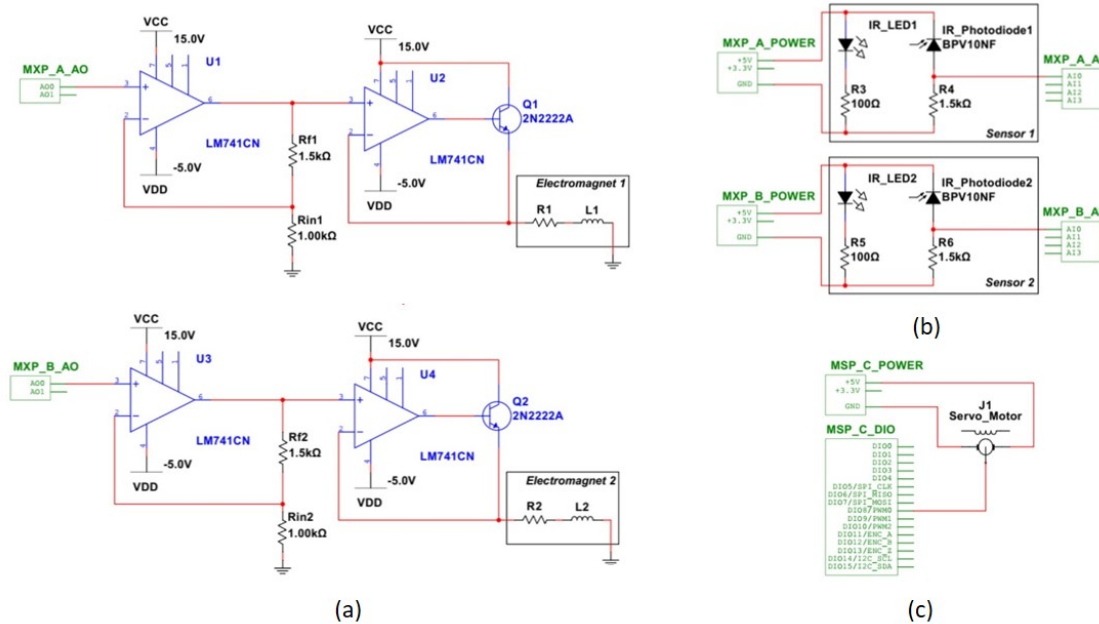

Figure 2. Schematic layout of (a) the MagLev system which consists of an amplifier circuit, (b) a sensor circuit, and (c) a servo motor which are all connected to an embedded NI myRIO board
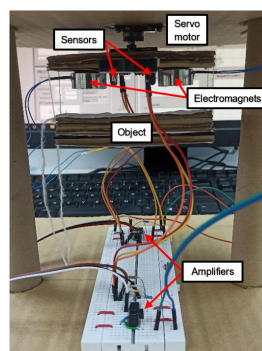

Figure 3. The MagLev system built in this study

2.2. Position control

To levitate the object to its equilibrium position, a correct amount of voltage is required to be supplied to the electromagnet. Figure 4 illustrates the experiment conducted to find the equilibrium position of the object (Figure 4(a)) and the LabVIEW VI (Figure 4(b)) where x denotes the distance from the IR emitter-receiver pair. In this study, the target object is of cuboid shape with dimension $10 \times 5 \times 2.5$ cm. The mass of the object is 23.7 g. The outputs of both the sensors are connected to the myRIO analog input, AI0 of connector ports A

and B. To measure and obtain the relationship between the object's position and the voltage from the sensors, a LabVIEW program is developed to log the data as depicted in Figure 4(b). The voltages of the sensors are recorded as the object is moved away from $x = 0.001$ to $x = 0.02$ m at a step of 0.001 m.
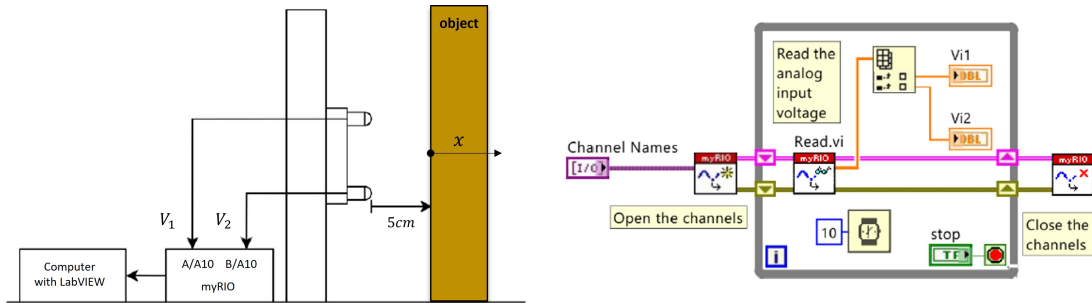

Figure 4. Illustration on the method to identify the equilibrium position where
(a) show experimental setup and (b) show block diagram of the LabVIEW VI

2.3. Orientation control

For the orientation control of the levitated object, the servo motor input is connected to a pulse-width modulation (PWM) channel with a frequency set at 50 Hz. However, it needs to be calibrated to nullify the offset reading from the servo motor input, y_p, which is -10 in this case. To calibrate it, the VI is run and the position is adjusted until the platform that the servo motor is attached to, which is defined as the orientation, becomes $0°$ relative to the plane. After the $0°$ is achieved, the position is recorded and set as the offset. A similar procedure is performed when the orientation is changed from $-90°$ to $+90°$. The line of best fit relating y_p to the orientation θ is obtained as (1):

$$y_p = 0.0014\theta^2 + 2.0611\theta, \quad \theta \in [-90, 90] \tag{1}$$

based on (1), the LabVIEW program is constructed as depicted in Figure 5 which shows the block diagram (Figure 5(a)) and the front panel (Figure 5(b)). The corresponding PWM and duty cycles are displayed on the front panel when the desired orientation is specified.
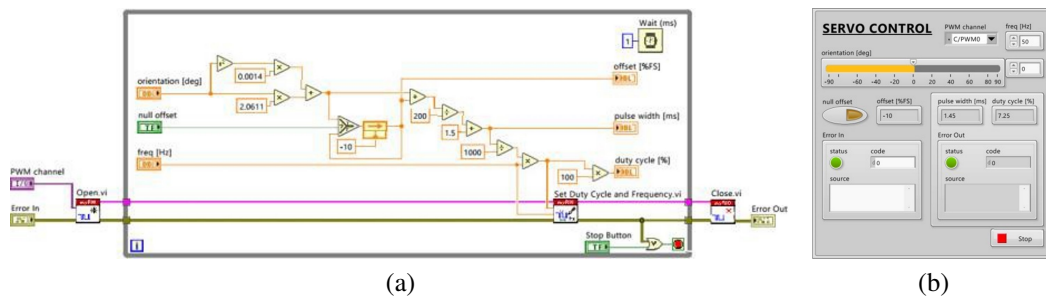

(a)   (b)

Figure 5. LabVIEW VI program for the orientation control of the MagLev
(a) the block diagram and (b) front panel

2.4. Feedback control

As the MagLev system is inherently nonlinear, a linearization at its equilibrium point has to be done in order to implement a feedback control system. From the preliminary experiment in section 2.2, the following equations are attained by applying a curve fitting method between $x = 0.009$ and $x = 0.011$ m, which are identified the equilibrium range of the system.

$$V_1 = -5.5x + 3.82; \quad V_2 = -5.4x + 3.84. \tag{2}$$

By setting $x_0 = 0.01$ m as the equilibrium position, the reference voltages for V_1 and V_2 obtained are 3.27 and 3.3 V respectively. To better visualize the motion of the levitated object, the relative values of V_1 and V_2, denoted as V_{s1} and V_{s2}, are used whose values are zero when the levitated object is at the equilibrium position. Therefore, V_{s1} and V_{s2} will fluctuate between negative and positive values when the levitated object fluctuates about the equilibrium position.

Let i_0 be the corresponding current when the object is at x_0, and L_0 be the additional inductance contributed by the presence of the levitated object at the equilibrium position. Figure 6 illustrates the structure of the linearized MagLev in a closed-loop with controller $G_c(s)$. The parameters of the MagLev are defined in Table 1 which are based on measurements and calculations. By taking V_s as the system's output, and the voltage supplied to the electromagnet, V_{in}, as the system's input, the open-loop transfer function of the MagLev can be written as (3):

$$G_p(s) = \frac{V_s(s)}{V_{in}(s)} = \frac{-\dfrac{2\beta_0 C i_0}{mLx_0^2}}{(s + \dfrac{R}{L})(s^2 - \dfrac{2Ci_0^2}{mx_0^3})} \tag{3}$$

where (4):

$$C = \frac{L_0 x_0}{2}; \quad L(x) = L_1 + \frac{L_0 x_0}{x}. \tag{4}$$

at the equilibrium point, we have $L = L_1 + L_0$. Substituting the parameters from Table 1 into (3), we will obtain (5):

$$G_p(s) = \frac{-9975}{(s + 185.4)(s^2 - 977.9)}. \tag{5}$$

let G_c be a PID controller with the following structure:

$$G_c(s) = k_p + \frac{k_i}{s} + k_d s \tag{6}$$

where k_p, k_i and k_d correspond to the proportional, integral and derivative gains respectively. The closed-loop transfer function can then be stated as follows:

$$T(s) = \frac{k_a G_c(s) G_p(s)}{1 + k_a G_c(s) G_p(s)} = \frac{ak_a(k_p s + k_i + k_d s^2)}{s(s + b)(s^2 + c) + ak_a(k_p s + k_i + k_d s^2)} \tag{7}$$

$$= \frac{ak_a k_d s^2 + ak_a k_p s + ak_a k_i}{s^4 + bs^3 + (c + ak_a k_d)s^2 + (bc + ak_a k_p)s + ak_a k_i} \tag{8}$$

where $a = -9975$, $b = 185.4$, and $c = -977.9$. A pole placement approach can be employed to tune the PID parameters by setting the desired characteristic equation as follows:

$$(s + p_1)(s + p_2)(s + 2\zeta\omega_n s + \omega_n^2) = 0 \tag{9}$$

with $p_1, p_2 > 0$, a settling time with 2% criterion of no more than 0.3 s, and a damping ratio of at least 0.8. These specifications will give us the following approximations:

$$4/\zeta\omega_n \approx 0.3, \leftrightarrow \zeta\omega_n \approx 13.3, \quad \therefore \omega_n \approx 16.625 \tag{10}$$

since the desired poles will be approximately located at $-13.3 \pm 9.93i$, the magnitudes of p_1, p_2 must be at least three times the magnitudes of the desired poles. Expanding (9) gives:

$$s^4 + [2\zeta\omega_n + p_1 + p_2]s^3 + [\omega_n^2 + 2(p_1 + p_2)\zeta\omega_n + p_1 p_2]s^2 + [(p_1 + p_2)\omega_n^2 + 2\zeta\omega_n p_1 p_2]s + p_1 p_2\omega_n^2 = 0. \tag{11}$$

comparing the left hand side of (11) with the denominator of (8), we can set $p_1 = 80$ and $p_2 = 79$ so that the characteristic equation becomes:

$$s^4 + 185.6s^3 + 10830s^2 + 212100s + 1747000 = 0 \tag{12}$$

equating the denominator of (8) with the left hand side of (12) gives.

$$c + ak_a k_d = 10830; \quad \leftrightarrow \quad k_d = -0.49 \tag{13}$$

$$bc + ak_a k_p = 212100; \quad \leftrightarrow \quad k_p = -16.43 \tag{14}$$

$$ak_a k_i = 1747000; \quad \leftrightarrow \quad k_i = -72.96 \tag{15}$$

In this work, both IR sensors are fed back, thus two PID controllers are required to compensate for the mismatches. The output from the controller, denoted by $V_{in} = [V_{in1} \quad V_{in2}]^T$, is then fed to the electromagnets as depicted in Figure 1.
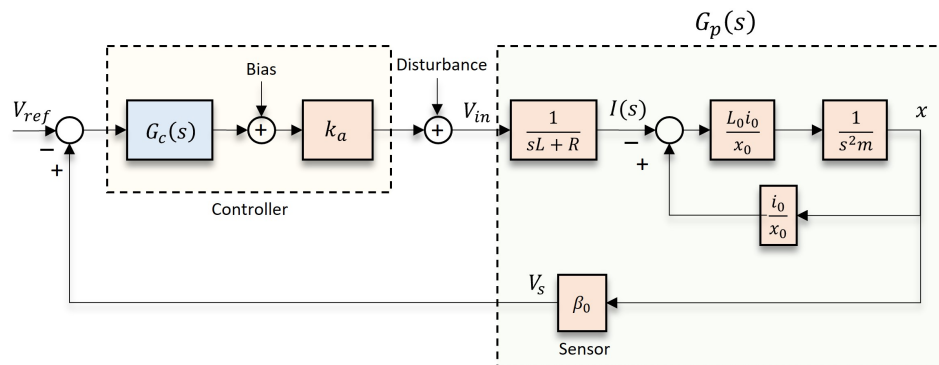
Figure 6. Illustration on the MagLev system with feedback control

Table 1. Parameters of the MagLev system

Notation	Definition	Value	Unit
g	Gravitational acceleration	9.81	ms^{-2}
m	Mass of the target object	0.0237	kg
R	Resistance of the electromagnet	72	Ω
L_1	Inductance of the electromagnet when there is no object levitated	0.05355	H
x_0	Equilibrium position	0.01	m
i_0	Current at the equilibrium position	0.0833	A
β_0	Position to voltage amplification coefficient	33	V/m
C	Constant that represents $L_0 x_0 / 2$	$1.674e^{-3}$	Hm
L_0	Additional inductance contributed by the presence of the levitated object	0.3348	H
k_a	amplification gain of the op-amp	2.4	

3. RESULTS AND DISCUSSION

The simulation results when the proposed PID controller is used are depicted in Figure 7. The step response in Figure 7(a) demonstrates that the 2% criterion for the settling time is met. Figure 7(b) shows the PID controller is able to stabilize the system when the initial position of the object is slightly displaced from its equilibrium position.

To verify the performance of the MagLev experimentally, the transient and steady-state responses of the system are recorded within the first 3 seconds with different initial conditions. Figure 8 illustrates the performance when the levitated object is at $0°$. The top plots (V_1 and V_2) refer to the controllers' outputs before being amplified to provide the right amount of currents to the electromagnets. The middle and bottom plots (V_{s1} and V_{s2}) correspond to the voltages from the IR sensors after being offset by 2.5 V; the red and blue lines refer to the actual and reference values respectively. From the plots, it can be observed that the steady state errors from V_{s1} and V_{s2} are within ± 1 V. As ± 3.3 V corresponds to ± 1 cm, the steady state voltage error of ± 1 V corresponds to a steady state position error of ± 0.3 cm.
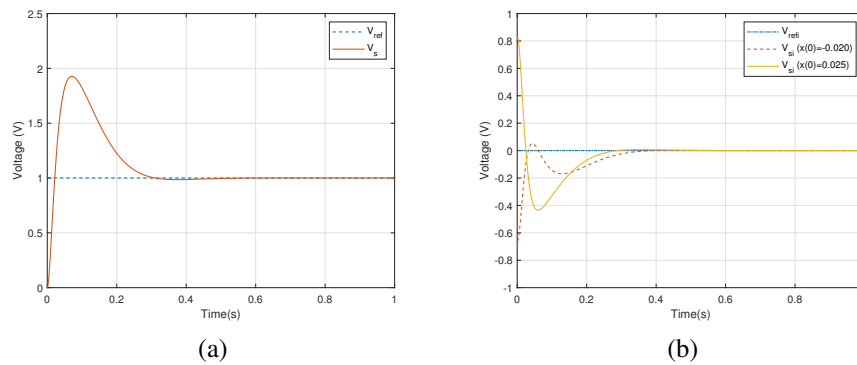
(a)   (b)

Figure 7. Simulation results for the MagLev system with the proposed PID controller (a) step response with the proposed PID controller and (b) time response with the relative voltage, V_{si}, and a initial values at non-equilibrium position, i.e. $x(0) \neq x_0$, to resemble the experimental setup
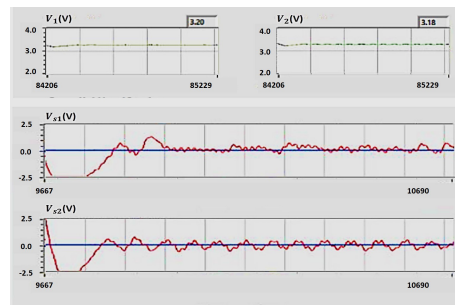

Figure 8. The transient and steady-state responses of the MagLev when the levitated object is at $0°$ with $x(0) = 0.02$ m

Figure 9 demonstrates the performance of the MagLev with the proposed position and orientation control strategy. The transient and steady-state responses of the MagLev when the levitated object rotates from $\theta = 0°$ to $\theta = 90°$, and from $\theta = 0°$ to $\theta = -90°$ are depicted in Figure 9(a) and Figure 9(b) respectively. For both cases, the initial position of the object was displaced from its equilibrium position; i.e. at $x = -0.02$ m for Figure 9(a) and $x = 0.025$ m for Figure 9(b). In Figure 9(a), the steady-state position error falls within ±0.3 cm after about 2 seconds of motion. Figure 9(b) shows a slightly larger steady-state position error which might be due to the larger initial displacement.
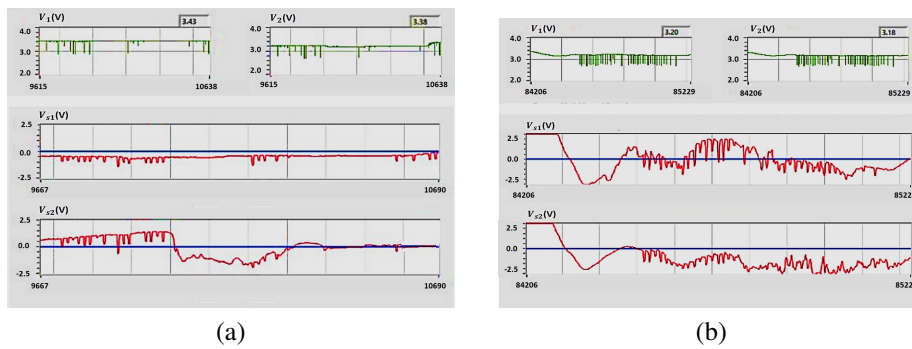

(a)   (b)

Figure 9. The transient and steady-state responses of the MagLev when the levitated object rotates from (a) $\theta = 0°$ to $\theta = 90°$ and (b) from $\theta = 0°$ to $\theta = -90°$

The numerical results for the three experiments are recorded in Table 2. From the table, it can be concluded that the proposed position and orientation control is able to drive the MagLev system to the desired conditions with steady-state position error of no greater than 1.2 cm. Figure 10 illustrates the experiments when the object is levitated and moved to $\theta = 0°$ (Figure 10(a)), $\theta = 90°$ (Figure 10(b)), and $\theta = -90°$ (Figure 10(c)).

Table 2. Numerical results from the experiments

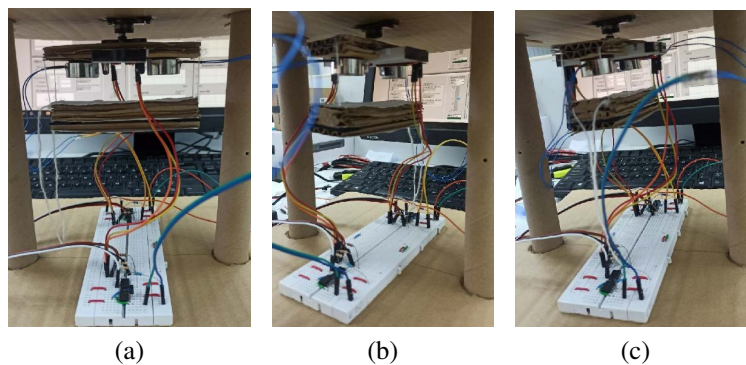| Exp.	Initial condition		Desired final condition		Steady-state error	
	x(m)	$\theta(°)$	x(m)	$\theta(°)$	$|\Delta x|$(m)	$|\Delta \theta|(°)$
1	0.020	0	0.01	0	0.003	0
2	-0.020	0	0.01	90	0.003	0
3	0.025	0	0.01	-90	0.012	0

(a)　　　　　　　　　　　　　(b)　　　　　　　　　　　　　(c)

Figure 10. Illustrations on the experiments when the object is levitated and moved to (a) $\theta = 0°$, (b) $\theta = 90°$, and (c) $\theta = -90°$

4. CONCLUSION

In this work, a MagLev system with position and orientation control has been successfully developed. Experimental results demonstrated that, with a non-zero initial displacement from equilibrium position, the proposed method was able to achieve a zero steady-state orientation error when the object was rotated from $0°$ to $\pm 90°$, a steady-state position error of 0.3 cm without rotation, and steady-state position errors of no greater than 1.2 cm with rotation.

Despite the achievements, the system is dependent on the size of the levitated object, i.e. it may not be able to work well for other objects with smaller sizes. In order to make the MagLev system more adaptive, future works will include additional actuators and sensors to form a cascade control loop which allows the system not just to identify the size of the object, but also modify the gap between the electromagnets in order to maintain the performance of the position and orientation control strategy. To further reduce the steady-state position error due to rotations, a state feedback control strategy may need to be employed to additionally control the current flowing through the coil. This method however requires an additional circuitry to sense the current and a modification on the control parameters to preserve the stability.

REFERENCES

[1]　G. Lin and X. Sheng, "Application and further development of maglev transportation in China," *Transportation Systems and Technology*, vol. 4, no. 3, pp. 36–43, 2018, doi: 10.17816/transsyst20184336-43.

[2]   A. Chaban, Z. Lukasik, M. Lis, and A. Szafraniec, "Mathematical modeling of transient processes in magnetic suspension of maglev trains," *Energies*, vol. 13, no. 24, p. 6642, 2020, doi: 10.3390/en13246642.

[3]   Y. He, J. Wu, G. Xie, X. Hong, and Y. Zhang, "Data-driven relative position detection technology for high-speed maglev train," *Measurement*, vol. 180, p. 109468, 2021, doi: 10.1016/j.measurement.2021.109468.

[4]   J. Xie, P. Zhao, C. Zhang, Y. Hao, N. Xia, and J. Fu, "A feasible, portable and convenient density measurement method for minerals via magnetic levitation," *Measurement*, vol. 136, pp. 564–572, 2019, doi: 10.1016/j.measurement.2019.01.005.

[5]   D. Tang, P. Zhao, Y. Shen, H. Zhou, J. Xie, and J. Fu, "Detecting shrinkage voids in plastic gears using magnetic levitation," *Polymer Testing*, vol. 91, p. 106820, 2020, doi: 10.1016/j.polymertesting.2020.106820.

[6]   S. Palagummi and F.-G. Yuan, "Magnetic levitation and its application for low frequency vibration energy harvesting," in *Structural Health Monitoring (SHM) in Aerospace Structures*, Elsevier, 2016, pp. 213–251, doi: 10.1016/B978-0-08-100148-6.00008-1.

[7]   K. Kecik and A. Mitura, "Theoretical and experimental investigations of a pseudo-magnetic levitation system for energy harvesting," *Sensors*, vol. 20, no. 6, p. 1623, 2020, doi: 10.3390/s20061623.

[8]   A. A. Ashkarran and M. Mahmoudi, "Magnetic levitation systems for disease diagnostics," *Trends in Biotechnology*, vol. 39, no. 3, pp. 311–321, 2021, doi: 10.1016/j.tibtech.2020.07.010.

[9]   S. M. Knowlton, B. Yenilmez, R. Amin, and S. Tasoglu, "Magnetic levitation coupled with portable imaging and analysis for disease diagnostics," *Journal of Visualized Experiments*, no. 120, Feb. 2017, doi: 10.3791/55012.

[10]   S. R. Dabbagh, M. M. Alseed, M. Saadat, M. Sitti, and S. Tasoglu, "Biomedical applications of magnetic levitation," *Advanced NanoBiomed Research*, vol. 2, no. 3, p. 2100103, 2022, doi: 10.1002/anbr.202100103.

[11]   H.-S. Han and D.-S. Kim, *Magnetic levitation*, vol. 13. Dordrecht: Springer Netherlands, 2016, doi: 10.1007/978-94-017-7524-3.

[12]   M. Ali and M. H. Miraz, "A review of underwater acoustic, electromagnetic and optical communications," in *Emerging Technologies in Computing. iCETiC 2020. Lecture Notes of the Institute for Computer Sciences, Social Informatics and Telecommunications Engineering*, Cham: Springer, 2020, pp. 86–97, doi: 10.1007/978-3-030-60036-5_6.

[13]   J. H. Teo, A. Loganathan, P. Goh, and N. S. Ahmad, "Autonomous mobile robot navigation via RFID signal strength sensing," *International Journal of Mechanical Engineering and Robotics Research*, pp. 1140–1144, 2020, doi: 10.18178/ijmerr.9.8.1140-1144.

[14]   S. Kishore and V. Laxmi, "Modeling, analysis and experimental evaluation of boundary threshold limits for Maglev system," *International Journal of Dynamics and Control*, vol. 8, no. 3, pp. 707–716, 2020, doi: 10.1007/s40435-020-00619-w.

[15]   Y. Sun, S. Wang, Y. Lu, and J. Xu, "Gaussian process dynamic modeling and backstepping sliding mode control for magnetic levitation system of maglev train," *Journal of Theoretical and Applied Mechanics*, pp. 49–62, Dec. 2021, doi: 10.15632/jtam-pl/143676.

[16]   I. Arrouch, N. S. Ahmad, P. Goh, and J. Mohamad-Saleh, "Close proximity time-to-collision prediction for autonomous robot navigation: an exponential GPR approach," *Alexandria Engineering Journal*, vol. 61, no. 12, pp. 11171–11183, 2022, doi: 10.1016/j.aej.2022.04.041.

[17]   N. S. Ahmad, J. H. Teo, and P. Goh, "Gaussian process for a single-channel EEG decoder with inconspicuous stimuli and eyeblinks," *Computers, Materials Continua*, vol. 73, no. 1, pp. 611–628, 2022, doi: 10.32604/cmc.2022.025823.

[18]   S. Yadav, S. K. Verma, and S. K. Nagar, "Optimized PID controller for magnetic levitation system," *IFAC-PapersOnLine*, vol. 49, no. 1, pp. 778–782, 2016, doi: 10.1016/j.ifacol.2016.03.151.

[19]   E. V. Kumar and J. Jerome, "LQR based optimal tuning of PID controller for trajectory tracking of magnetic levitation system," Procedia Engineering, vol. 64, pp. 254–264, 2013, doi: 10.1016/j.proeng.2013.09.097.

[20]   A. V. Starbino and S. Sathiyavathi, "Design of sliding mode controller for magnetic levitation system," *Computers Electrical Engineering*, vol. 78, pp. 184–203, Sep. 2019, doi: 10.1016/j.compeleceng.2019.07.007.

[21]   P. Roy and B. K. Roy, "Sliding mode control versus fractional-order sliding mode control: applied to a magnetic levitation system," *Journal of Control, Automation and Electrical Systems*, vol. 31, no. 3, pp. 597–606, 2020, doi: 10.1007/s40313-020-00587-8.

[22]   N. S. Ahmad, "Robust H_∞-fuzzy logic control for enhanced tracking performance of a wheeled mobile robot in the presence of uncertain nonlinear perturbations," *Sensors*, vol. 20, no. 13, p. 3673, 2020, doi: 10.3390/s20133673.

[23]   B. Ataşlar-Ayyıldız, O. Karahan, and S. Yılmaz, "Control and robust stabilization at unstable equilibrium by fractional controller for magnetic levitation systems," *Fractal and Fractional*, vol. 5, no. 3, p. 101, 2021, doi: 10.3390/fractalfract5030101.

[24]   A. Mughees and S. A. Mohsin, "Design and control of magnetic levitation system by optimizing fractional order PID controller using ant colony optimization algorithm," *IEEE Access*, vol. 8, pp. 116704–116723, 2020, doi: 10.1109/ACCESS.2020.3004025.

[25]   T. Tariq and V. Mehmet, "Control of single axis magnetic levitation system using fuzzy logic control," *International Journal of Advanced Computer Science and Applications*, vol. 4, no. 11, 2013, doi: 10.14569/IJACSA.2013.041111.

[26]   J. Tang, Z. Huang, Y. Zhu, and J. Zhu, "Neural network compensation control of magnetic levitation ball position based on fuzzy inference," *Scientific Reports*, vol. 12, no. 1, p. 1795, 2022, doi: 10.1038/s41598-022-05900-w.

[27]   I. Arrouch, J. M. Saleh, P. Goh, and N. S. Ahmad, "A comparative study of artificial neural network approach for autonomous robot's TTC prediction," *International Journal of Mechanical Engineering and Robotics Research*, pp. 345–350, 2022, doi: 10.18178/ijmerr.11.5.345-350.

[28]   C. H. Goay, P. Goh, N. S. Ahmad, and M. F. Ain, "Eye-height/width prediction using artificial neural networks from s-parameters with vector fitting," *Journal of Engineering Science and Technology*, vol. 13, no. 3, pp. 625-639, 2018.

[29]   J. H. Teo, N. S. Ahmad, and P. Goh, "Visual stimuli-based dynamic commands with intelligent control for reactive BCI applications," *IEEE Sensors Journal*, vol. 22, no. 2, pp. 1435–1448, 2022, doi: 10.1109/JSEN.2021.3130626.

[30]   A. K. Sahoo, S. K. Mishra, B. Majhi, G. Panda, and S. C. Satapathy, "Real-time identification of fuzzy PID-controlled maglev system using TLBO-based functional link artificial neural network," *Arabian Journal for Science and Engineering*, vol. 46, no. 4, pp. 4103–4118, 2021, doi: 10.1007/s13369-020-05292-x.

[31]   D. Sain and B. M. Mohan, "Modelling of a nonlinear fuzzy three-input PID controller and its simulation and experimental realization," *IETE Technical Review*, vol. 38, no. 5, pp. 479–498, 2021, doi: 10.1080/02564602.2020.1773326.

[32]   B. Ataşlar-Ayyıldız and O. Karahan, "Design of a MAGLEV system with PID based fuzzy control using CS algorithm," *Cybernetics and Information Technologies*, vol. 20, no. 5, pp. 5–19, 2020, doi: 10.2478/cait-2020-0037.

[33] J. J. Rubio, L. Zhang, E. Lughofer, P. Cruz, A. Alsaedi, and T. Hayat, "Modeling and control with neural networks for a magnetic levitation system," *Neurocomputing*, vol. 227, pp. 113–121, 2017, doi: 10.1016/j.neucom.2016.09.101.

[34] A. B. Subramaniam *et al.*, "Noncontact orientation of objects in three-dimensional space using magnetic levitation," *Proceedings of the National Academy of Sciences*, vol. 111, no. 36, pp. 12980–12985, 2014, doi: 10.1073/pnas.1408705111.

[35] J. Xie, P. Zhao, C. Zhang, J. Fu, and L.-S. Turng, "Current state of magnetic levitation and its applications in polymers: a review," *Sensors and Actuators B: Chemical*, vol. 333, p. 129533, Apr. 2021, doi: 10.1016/j.snb.2021.129533.

BIOGRAPHIES OF AUTHORS

Siti Juliana Abu Bakar 🆔 📛 📊 ↻ received her B.Eng degree (Hons.) in electronic engineering from UTeM, Malaysia in 2019 and Master ESDE (Electronic System Design Engineering) from USM, Malaysia, in the year 2015. Completed her Ph.D. in the field of Automation and Control System from Universiti Sains Malaysia, Engineering Campus in 2020. She is currently working as senior lecturer at Centre for Electrical Engineering Studies, Universiti Teknologi MARA Campus Pulau Pinang Malaysia. Prior working as a senior lecturer at UiTM, she worked at Intel Product (M) Sdn.Bhd more than 5 years as Validation Engineer. She can be contacted at email: sitijuliana@uitm.edu.my.

Koay J-Shenn 🆔 📛 📊 ↻ was born in Penang in 1998. He received the B.Eng. degree in electronic engineering from School of Electrical and Electronic Engineering, Universiti Sains Malaysia (USM) in 2022. His research interest centers around automation and control systems. In 2021, he joined National Instruments as an intern working on software-based projects. He is currently working as an electrical engineer in Penang. He can be contacted at email: koayjshenn71@student.usm.my.

Patrick Goh 🆔 📛 📊 ↻ received the B.S., M.S., and Ph.D. degrees in electrical engineering from the University of Illinois at Urbana-Champaign, Urbana, IL, USA in 2007, 2009, and 2012 respectively. Since 2012, he has been with the School of Electrical and Electronic Engineering, Universiti Sains Malaysia, where he currently specializes in the study of signal integrity for high-speed digital designs. His research interest includes the development of circuit simulation algorithms for computer-aided design tools. He was a recipient of the Raj Mittra Award in 2012 and the Harold L. Olesen Award in 2010, and has served on the technical program committee and international program committee in various IEEE and non-IEEE conferences around the world. He can be contacted at email: eepatrick@usm.my.

Nur Syazreen Ahmad 🆔 📛 📊 ↻ received the B.Eng. degree in Electrical and Electronic Engineering from the University of Manchester, United Kingdom and Ph.D. degree in Control Systems from the same university. She is currently an Associate Professor at the School of Electrical and Electronic Engineering, University Sains Malaysia (USM), specializing in embedded control systems, sensor networks and mobile robotics. Her main research interest revolves around autonomous mobile robots, with a particular focus on sensing, identification, intelligent control and indoor navigation. She is a member of the IEEE Young Professional and Control System societies, and has gained a recognition as a Certified LabVIEW Associate Developer by NI. She can be contacted at email: syazreen@usm.my.